Trajectory Design of Formation Flying Constellation for Space-Based Solar Power

Ashish Goel
Graduate Aerospace Laboratories of the California Institute of Technology
Pasadena, CA 91125
650-804-4689
ashishg@caltech.edu

Nicolas Lee
Department of Aeronautics and Astronautics
Stanford University
Stanford, CA 94305
650-723-9564
nnlee@stanford.edu

Sergio Pellegrino
Graduate Aerospace Laboratories of the California Institute of Technology
Pasadena, CA 91125
626-395-4764
sergiop@caltech.edu

***Abstract*—The concept of collecting solar power in space and transmitting it using microwaves has appealed to the imagination of numerous aerospace researchers in the past. The Space Solar Power Initiative at Caltech is working towards turning this idea into reality, by developing the critical technologies necessary to make this an economically feasible solution. The proposed system comprises an array of ultra-light, membrane-like deployable modules with high efficiency photovoltaics and microwave transmission antennas embedded in the structure. Each module is 60 m X 60 m in size and in the final configuration, ~2500 of these modules span a 3 km X 3 km array in the geostationary orbit.**

As the constellation goes around the Earth, the orientation and position of each module has to be changed so as to optimize the angle made by the photovoltaic surface with respect to the sun and by the antenna surface with respect to the receiving station on Earth. We derive the optimum orientation profile for the modules and find that modules with dual-sided RF transmission can provide 1.5 times more orbit-averaged power than modules with single-sided RF transmission. To carry out the corresponding orbital maneuvers, an optimization framework using the Hill-Clohessy-Wiltshire (HCW) equations is developed to achieve the dual goal of maximizing the power delivered, while minimizing the propellant required to carry out the desired orbital maneuvers. Results are presented for a constellation with modules in fixed relative positions and also for a constellation where the modules execute circularized periodic relative motion in the HCW frame. We show that the use of these periodic relative orbits reduces the propellant consumption by more than a factor of 2, thereby solving a major technical hurdle in the realization of space-based solar power.

TABLE OF CONTENTS

978-1-5090-1613-6/17/31.00 ©2017 IEEE

1. INTRODUCTION

The concept of collecting solar power in space and transmitting it using microwaves was initially floated in a science fiction magazine by Isaac Asimov [1] and first proposed in a technical paper by Glaser in 1968 [2]. Since then, numerous researchers have worked on architectures and implementation strategies for realizing the dream of space-based solar power. The biggest advantage of space-based solar power over terrestrial systems is the independence from diurnal and seasonal cycles which further alleviates the need for expensive storage solutions. Significantly more solar power can be collected in space without atmospheric losses and interruptions from changing weather patterns. Further, microwave power from space can be beamed on-demand to any location on Earth, irrespective of its latitude. This enables the supply of clean renewable energy to resource-starved areas on Earth.

The Space Solar Power Initiative (SSPI) at Caltech is a collaborative project to bring about the scientific and technological innovations necessary for enabling a space-based solar power system. The proposed system comprises an array of ultra-light, membrane-like deployable modules with high efficiency photovoltaic (PV) systems and microwave transmission antennas embedded in the structure. Each module is 60 m X 60 m in size and in the final configuration, hundreds of these modules span a 3 km X 3 km array in a geosynchronous orbit. This architecture is depicted in Fig. 1, reproduced from [3].

One of the primary challenges for the SSPI project is the design and maintenance of a satellite constellation in formation flight. In the past decade, substantial amount of research has been done on the guidance, navigation and control of formation flying satellites [4–7]. Formation flight has also been demonstrated in space by missions such as GRACE

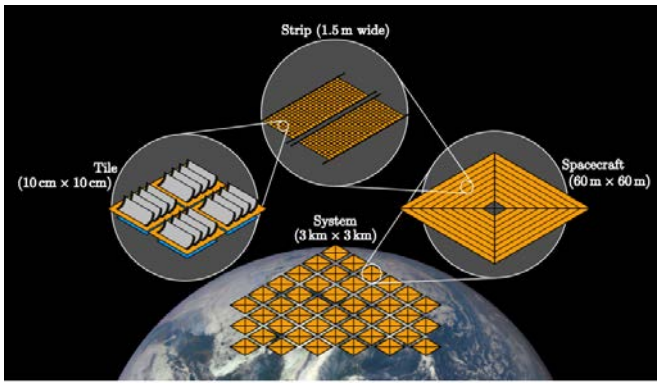

Figure 1. Overview of Space Solar Power System.

[8], GRAIL [9], TanDEM-X [10] and PRISMA [11]. In this paper, our goal is to leverage some of these recent advancements for the trajectory design of this formation-flying constellation.

Each module in the constellation is made up of a large number of 'tiles'. The tile is the fundamental unit of this design and comprises two primary layers. The top layer contains a series of parabolic concentrators. Solar radiation incident on these concentrator mirrors gets directed towards a thin strip of photovoltaic cells located on the back side of the concentrators. The DC photocurrent is then converted into microwave radiation at 10 GHz frequency with RF electronic ICs located on the undersides of the top layer. Patch antennas located on the bottom layer of the tile radiate the RF power towards an array of rectifying antennas (rectennas) on Earth. Precision timing control at each of the patch antennas allows us to operate them in the form of a phased array to carry out beam-forming and beam-steering, thereby directing the power towards desired locations on Earth.

As a modification to this baseline design, one can add an additional layer of PV-transparent antennas on top, or equivalently, RF-transparent PV on the bottom to allow dual-sided operation of the module. As discussed in Section 2, this can significantly improve the performance of the module in orbit. For the baseline design discussed in this paper, we assume that the constellation is in the geostationary orbit so that all the power can be transmitted instantaneously to a single receiving station on Earth. To recover the launch costs, the modules are designed to operate in orbit for a duration of 11 years.

Historically, one of the biggest financial hurdles to the idea of space-based solar power has been the enormous cost associated with placing such an array in orbit. Therefore, reducing the mass of the system is critical to making space-based solar an economically feasible idea. The SSPI concept is addressing this challenge by using ultra-thin deployable structures which reduces the total dry mass of a module to an extremely low value of ~370 kg. The work presented in this paper is therefore driven by the motivation to keep the propellant mass down to a small fraction of this dry mass.

As the constellation goes around the Earth, the orientation and position of each module has to be changed so as to optimize the angle made by the photovoltaic surface with respect to the sun and by the antenna surface with respect to the receiving station on Earth. The problem is exacerbated by the presence of strong perturbation from solar radiation pressure due to the high area to mass ratio of the modules. In Section 2 of this paper, we discuss the optimum orientation of each module at different locations in the orbit. For the analysis presented in this section, we focus on a single module in the constellation. In Section 3, we discuss how the orientation requirement translates into a requirement for orbital maneuvering of the modules. We then present an outline of the optimization framework under which we design such orbital maneuvers. In Section 4, we present the results from our analysis for the worst case module which is farthest away from the reference geostationary orbit. A brief discussion and our conclusions are presented in Sections 5 and 6 respectively.

2. OPTIMUM MODULE ORIENTATION

For any orbital position of the module (θ), the total power delivered to the receiving station on Earth depends on two primary geometrical factors:

1. The dependence of photovoltaic efficiency on the angle made by the module with respect to the sun (β). This dependency P(θ), which is obtained using ray-tracing simulations of the concentrators, is plotted in Fig. 2a.
2. The dependence of RF efficiency on the angle made by the module with respect to the receiving station on Earth (ϕ). There are two components to this dependency.
- R(ϕ): The variation of the radiation pattern of a single patch antenna with ϕ and
- AF(ϕ): The variation of the array factor with ϕ ($cos\phi$)

The patch antennas on the module are near-isotropic and the variation of the efficiency of one such antenna in the array is plotted in Fig. 2b. The array efficiency is simply assumed to vary as the area projected by the array at the receiving station.

Due to the planar design of the module, the angles β and ϕ are not independent. They are geometrically related to the orbital angle θ, as illustrated in Fig. 3.

$$\theta = \beta + \phi \tag{1}$$

For every orbital position θ, we treat β as the independent variable and calculate the value of ϕ using Equation 1. We then compute the total geometrical efficiency ($G(\beta, \phi)$) by multiplying the various RF and PV efficiencies listed above.

$$G(\beta, \phi) = P(\beta) \times R(\phi) \times cos(\phi) \tag{2}$$

For every orbital position θ, we can now compute $G(\beta, \phi)$ for different values of β to arrive at the optimum value of β. This calculation is carried out for the case of both single-sided and dual-sided modules and the results obtained are pictorially represented in Fig. 4. The optimum orientation for the two profiles are identical until we reach the orbital angle of 90 degrees. In the single-sided case, the value of β keeps increasing while in the dual-sided case, we can now flip the module and start using the antenna on front side to keep the geometrical efficiency high. In the single sided case, we eventually reach a point where the value of the steering angle (β) becomes so high that no power can be transmitted to Earth. On the other hand, a dual-sided module allows the geometrical efficiency value to remain above 0.5 throughout the orbit.

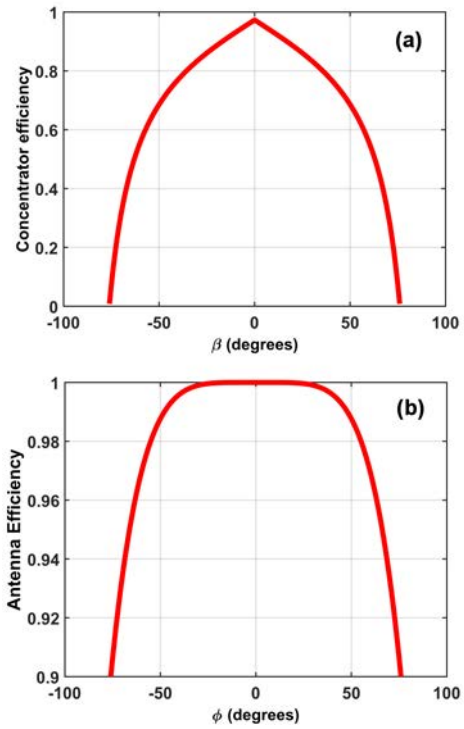

Figure 2. (a) Variation of concentrator efficiency with angle β (b) Variation of efficiency of an antenna in the phased array with angle ϕ. Both these variations are symmetric for positive and negative values of respective angles.

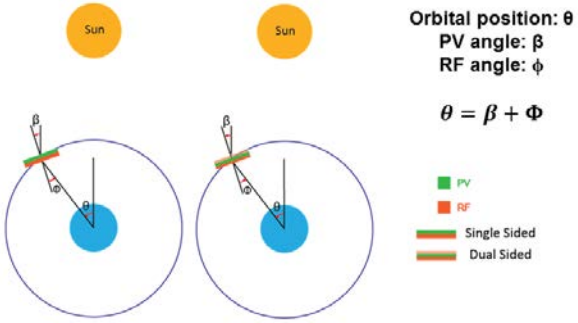

Figure 3. Single-sided and dual-sided modules in orbit around the Earth, showing various angles relevant to estimating the overall efficiency of the system.

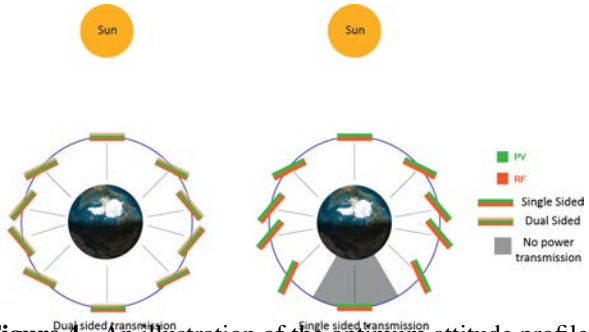

Figure 4. An illustration of the optimum attitude profile for both singe-sided and dual-sided modules.

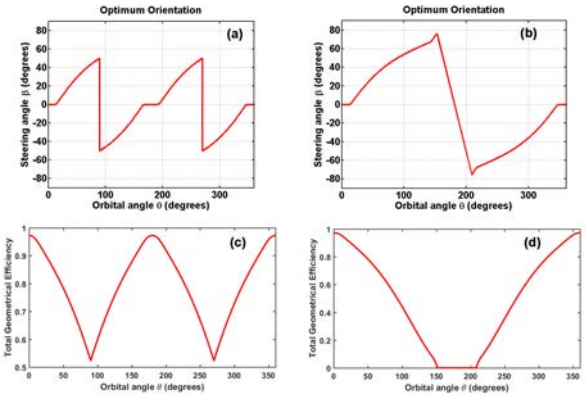

Figure 5. (a) Optimum attitude profile for the dual-sided module (b) Optimum attitude profile for the single-sided module (c) Geometric efficiency variation for the dual-sided module (d) Geometric efficiency variation for the single-sided module.

The optimum attitude profiles and associated geometrical efficiency values for the dual-sided and single-sided cases are shown graphically in Fig. 5. Using these efficiency values, we can now compute the orbit-averaged power density (OAP) transmitted to Earth. For this calculation, we assume the solar constant to be 1361 W/m^2, a PV efficiency of 0.30 and a DC-RF conversion efficiency of 0.78. We ignore the losses due to the 23.5° angle between the ecliptic plane and Earth's equatorial plane. Using these numbers, we arrive at an OAP of 252 W/m^2 for the dual-sided case and 155 W/m^2 for the single-sided module. This result is critical since it dictates a crucial decision in the design of the module. While a single-sided module is lighter and requires simpler maneuvers in orbit, it gives almost 0.6 times less power than the dual-sided module. In order to compete with terrestrial solar farms, it is imperative that we use dual-sided modules. Hence for the orbital analysis in Section **??**, we focus on results only for dual-sided modules.

In the dual-sided case, practically speaking, the flipping maneuver at $\theta = 90°$ and $\theta = 270°$ has to be carried out over a finite range of angles. While it makes the system go through a temporary phase of low geometrical efficiency, the slower this maneuver, the lesser the amount of burden on the attitude control system. It also reduces the propellant needed for orbital maneuvers, as we shall see in Section 4. If this maneuver is carried out over an orbital angle of 20 degrees (80 minutes maneuver), it only reduces the OAP from 252 W/m^2 to 249 W/m^2.

In order to carry out these maneuvers, we propose to deploy attitude control thrusters located at the corners of the module. We assume that these thrusters have a specific impulse of 3000 s, based on the numbers reported by various groups working on miniaturized, state-of-the-art electric propulsion systems [12–15]. Using a propellant-minimizing attitude control scheme, we calculate the total propellant mass required over 11 years to be 2.16 kg for the dual-sided case and 0.84 kg for the single sided module. The corresponding thrust profiles of the attitude control thrusters can be seen in Fig. 6. As expected, more fuel is needed for the sharp maneuvers of the dual-sided modules but in either case, the total fuel requirement is a very small number compared to the mass of the module.

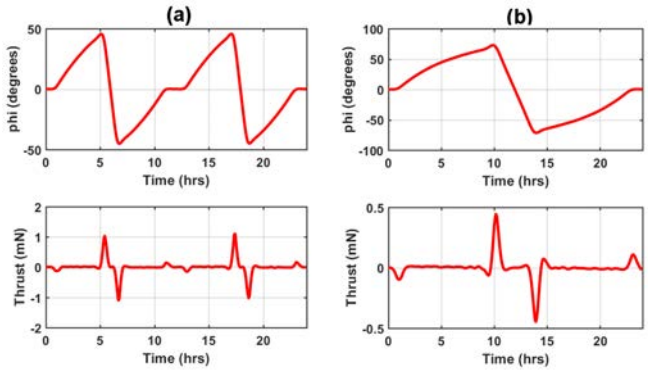

Figure 6. (a) Optimum attitude and thrust profiles for dual-sided module with the flip carried out over an orbital angle of 20 degrees b) Optimum attitude and thrust profiles for single-sided module.

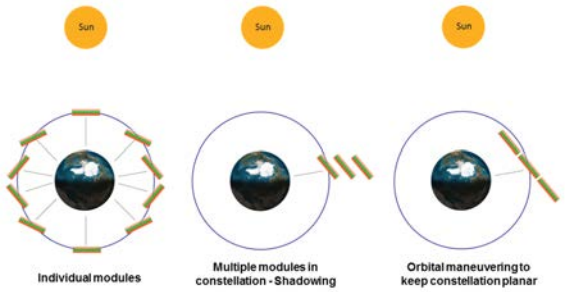

Figure 7. An illustration of why relative orbital motion among the modules is necessary to prevent the modules from obstructing each other.

3. Orbital Maneuvering for Optimum Power Transfer

The analysis presented in Section 2 was considering a single isolated module. When we consider an array of modules, if the modules are simply rotated in their respective positions, the modules would start blocking/shadowing each other, as depicted in Fig. 7. In order to avoid this, one simple solution is to have every attitude maneuver accompanied by a corresponding orbital maneuver to ensure that the constellation remains planar.

In order to analyze these orbital maneuvers and to come up with an optimal maneuvering profile, an optimization framework is developed using the Hill-Clohessy-Wilthire (HCW) equations [16] shown below.

$$\underbrace{\begin{bmatrix} \dot{x} \\ \dot{y} \\ \dot{z} \\ \ddot{x} \\ \ddot{y} \\ \ddot{z} \end{bmatrix}}_{\dot{s}} = \underbrace{\begin{bmatrix} 0 & 0 & 0 & 1 & 0 & 0 \\ 0 & 0 & 0 & 0 & 1 & 0 \\ 0 & 0 & 0 & 0 & 0 & 1 \\ 3n^2 & 0 & 0 & 0 & 2n & 0 \\ 0 & 0 & 0 & -2n & 0 & 0 \\ 0 & 0 & -n^2 & 0 & 0 & 0 \end{bmatrix}}_{D} \underbrace{\begin{bmatrix} x \\ y \\ z \\ \dot{x} \\ \dot{y} \\ \dot{z} \end{bmatrix}}_{s} + \underbrace{\begin{bmatrix} 0 & 0 & 0 \\ 0 & 0 & 0 \\ 0 & 0 & 0 \\ 1 & 0 & 0 \\ 0 & 1 & 0 \\ 0 & 0 & 1 \end{bmatrix}}_{C} \underbrace{\begin{bmatrix} f_x \\ f_y \\ f_z \end{bmatrix}}_{u} \tag{3}$$

For computing purposes, this continuous time linear dynamical system (LDS) can be transformed into a discrete time LDS as per the following equation

$$\dot{s} = Ds + Cu \tag{4}$$

$$s(t+1) = As(t) + Bu(t) \tag{5}$$

where $A = e^{hD}$ and $B = (\int_0^h e^{\tau D} d\tau)C$ and h is the discretization time step, chosen to be 20 minutes for this analysis. The inherent dynamics of the system operate at the time-scale of the synodic period (1 day). The quantity $u(t)$ in equation 5 represents the thrust-per-unit-mass vector, which is assumed to be constant from time t to $t+1$. We can now express every state from initial state to final state as a linear combination of the initial state and the forces applied during each time step, as shown below.

$$\begin{aligned} s(1) &= As(0) + Bu(0) \\ s(2) &= As(1) + Bu(1) \\ s(2) &= A^2 s(0) + ABu(0) + Bu(1) \\ &\vdots \\ s(N) &= A^N s(0) + A^{N-1}Bu(0) + A^{N-2}Bu(1) + \ldots + Bu(N-1) \end{aligned}$$

These equations can be expressed in matrix form as

$$\underbrace{\begin{bmatrix} s(N) \\ s(N-1) \\ s(N-2) \\ \vdots \\ s(1) \end{bmatrix}}_{S} = \underbrace{\begin{bmatrix} B & AB & A^2B & \ldots & A^{N-1}B \\ 0 & B & AB & \ldots & A^{N-2}B \\ 0 & 0 & B & \ldots & A^{N-3}B \\ \vdots & & & & \vdots \\ 0 & 0 & 0 & \ldots & B \end{bmatrix}}_{P} \underbrace{\begin{bmatrix} u(N-1) \\ u(N-2) \\ u(N-3) \\ \vdots \\ u(0) \end{bmatrix}}_{U} + \underbrace{\begin{bmatrix} A^N \\ A^{N-1} \\ A^{N-2} \\ \vdots \\ A \end{bmatrix}}_{Q} s_0 \tag{6}$$

$$S = PU + Qs_0 \tag{7}$$

The optimization problem can now be formulated as

variables $\mathbf{U}$, $\boldsymbol{\beta}$

minimize $\quad ||U||_p - \lambda f_{OAP}(\boldsymbol{\beta})$

subject to $\quad PU + Qs_0 = S_{des} = g(\boldsymbol{\beta})$

f_{OAP} is a function which calculates the orbit-averaged power density for any given attitude profile. λ is a parameter that determines the relative weightage between propellant mass and power transmitted. If λ is 0, the cost function minimizes the total norm of the thrust vector, thereby minimizing the propellant mass. If λ is ∞, it maximizes the transmitted power irrespective of the propellant mass needed to carry out those maneuvers. These maneuvers for $\lambda = \infty$ correspond to the optimum attitude profile shown in Fig. 5. By varying this parameter lambda over a wide range of values, we can study the trade-off between propellant mass and transmitted power to generate the Pareto optimal curve. Note that this cost function can be modified to include other considerations such as minimizing maximum thrust, maximizing minimum transmitted power over one orbit etc.

The constraint equation incorporates the dynamics of the HCW equations and the function $g(\beta)$ can be used to impose planarity and other restrictions on the structure of the constellation. In the following sections, we discuss a few different alternatives for the choice of β and show the resulting Pareto optimal curves obtained by solving the optimization problem. Note that the presence of $g(\beta)$ and $f_{OAP}(\beta)$ makes the problem non-convex. We solve the problem numerically using the Sparse Non-Linear Optimization (SNOPT) toolkit [17].

Applicability of HCW Equations

There are 3 major assumptions that allow the use of the HCW formulation

1. The reference orbit is circular
2. There are no perturbation forces
3. The distance of the module from the reference orbit is small compared to the distance of the reference orbit from the central body (Earth)

The third assumption clearly holds since the size of the constellation is significantly small compared to the size of the geostationary orbit. But since the modules have extremely high area-to-mass ratio, there can be a significant perturbation force due to solar radiation pressure (SRP). The primary effect of SRP is to ellipticize the orbit of the modules. This effect is illustrated in Fig. 8. The degree of ellipticization is captured by the following set of equations [18, 19]

$$\begin{aligned} C &= \frac{3}{2}\frac{n_M}{n_P}\frac{a_{SRP}}{a_{gP}} \\ e &= \frac{C}{\sqrt{1+C^2}} \end{aligned} \tag{8}$$

Here e is the eccentricity of the ellipticized orbit, a_{SRP} is the acceleration due to solar radiation pressure, a_{gP} is the gravitation acceleration from the central body (Earth), n_M is the mean motion of the module and n_P is the mean motion of the central body (mean motion of Earth around the sun). For the current areal mass density of our modules, the eccentricity of the orbit due to solar radiation pressure is 0.11. When the eccentricity is small ($e < 0.3$), the HCW equations can be

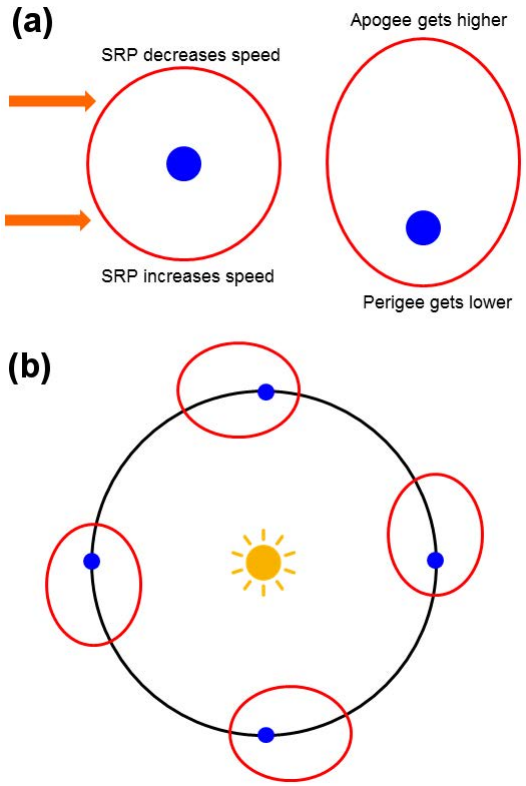

Figure 8. (a) An illustration of solar radiation pressure causing ellipticization of the orbit (b) An illustration showing the major axis of this non-Keplerian elliptical orbit rotating as the Earth goes around the sun.

modified to incorporate the effects of non-zero eccentricity by using a power series expansion in terms of e [20]. The degree of the power series can be chosen based on the level of accuracy desired. In the state space representation, this leaves us with a linear time-varying dynamical system, making the equations significantly more complex. An alternative would be to formulate the problem in the form of relative orbital elements. This gives us more accurate results without limiting us to low-eccentricity orbits but the equations become non-linear, thereby preventing us from using the simple state space representation described in equation 5. For the analysis presented in this paper, we ignore the effects of solar radiation pressure. These effects will be incorporated in the future, once we have a better handle on the areal mass density of our modules.

4. RESULTS

Rectangular Grid with Fixed Relative Positions

From an operational standpoint, one of the simplest choices for the constellation would be to have all the modules in a planar rectangular grid with fixed relative positions. The entire plane of modules would rotate about an axis parallel to the rotation axis of the Earth (z-axis in the HCW frame) to optimize power collection and transmission but the relative position of every module in the plane is fixed. An illustration of this architecture in the inertial frame of reference can be seen in Fig. 9. Note that this figure is not to scale. The modules have been placed in an orbit much closer than the geostationary orbit to enable visualization. We impose

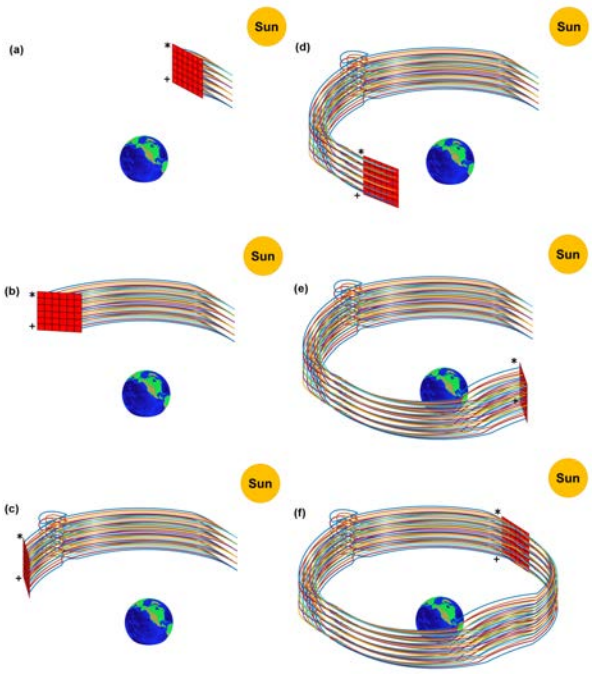

Figure 9. Orbits of a 6×6 constellation with fixed relative positions of modules within the plane of the rectangular array. The positions of two of the modules are marked with $*$ and $+$ to help track their positions. These plots are from the point of view of an inertial observer over 24 hours. Note that the sizes of elements in this figure are not representative of their actual sizes.

this orbital behavior on the modules through $g(\beta)$ and the resulting Pareto optimal curve can be seen in Fig. 10.

Just to reiterate, this curve has been obtained for the worst-case, dual-sided module located at the corner of the 3 km×3 km constellation. The mission duration is assumed to be 11 years, the dry mass of the module is 370 kg and the Isp of the thruster is assumed to be 3000 s. From Fig. 10, we infer that in order to achieve power levels close to the maximum value of 252 W/m^2, the modules have to carry in excess of 150 kg of propellant, which is greater than 1/3rd the mass of the module itself.

Periodic Relative Orbits

The primary reason why the solution described above requires large amount of propellant mass is because we are forcing the modules to stay in fixed relative positions with respect to the reference orbit. For instance, a module starting with a positive value of z in the HCW frame is forced to maintain the same value of z throughout the orbit. However, in the absence of a forcing function, the modules would naturally tend to execute periodic motion around the reference orbit. If the energy matching condition is met [7], the modules would go around the reference orbit in closed orbits called periodic relative orbits (PROs). These concentric PROs represent propellant-less solutions for a formation-flying constellation. The initial conditions for generating these PROs in the HCW (local vertical local horizontal - LVLH) frame are [21]:

$$\begin{aligned} \dot{x_0} &= \tfrac{1}{2} n y_0 \\ \dot{y_0} &= -2 n x_0 \end{aligned} \tag{9}$$

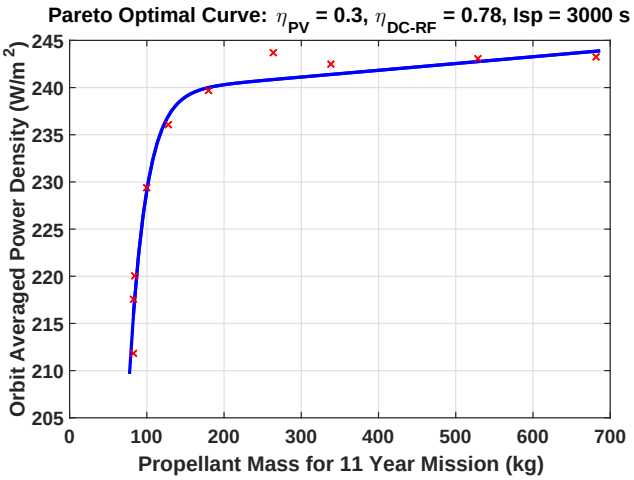

Figure 10. Pareto optimal curve for the worst case module in a constellation where the modules are at fixed relative positions within the plane of the constellation. As fuel mass increases, we reach the upper limit of 252 W/m^2, as discussed in Section 2. In order to achieve power density values close to the upper limit, we need propellant mass greater than 1/3rd the mass of the module.

The equation for the z-direction is decoupled from the x and y equations and the initial conditions for z_0 and $\dot{z_0}$ can be chosen to realize different PROs with the same projections in the x-y plane. As can be seen from Equation 9, PROs represent elliptical solutions that are not ideal for the SSPI constellation. If we provide the right set of initial conditions, as per Equation 9, for two modules that are initially separated by a distance of 60 m and track the inter-module distance over a period of one orbit, we find that this distance varies significantly with time. This can be seen in Fig. 11. The power transmission efficiency of the phased array diminishes significantly as the modules deviate away from their ideal positions. Therefore, forces have to be applied on these modules to circularize their orbits and to rotate their orbital planes as per the desired attitude profile. Once these requirements are incorporated in the optimization framework ($g(\beta)$), the resulting orbits, as viewed from an inertial frame of reference, can be seen in Fig. 12.

The Pareto optimal curve obtained for this PRO-based solution is shown in Fig. 13. Typically, one chooses an operating point on the knee of this curve. Comparing these results to those shown in Fig. 10, we can see that using PROs offers a significant advantage in terms of propellant mass required for the same orbit-averaged power.

5. Discussion and Future Work

The results presented in Section 4 have been obtained for the module farthest away from the reference orbit, at the corner of the constellation. For the same transmitted power, less propellant is required for modules that are closer to the reference orbit. This effect is captured in Fig. 14. For a module in the geostationary orbit, only attitude maneuvers are needed for optimum power transmission and the mass of the propellant required increases almost linearly with increasing distance from the geostationary orbit. One of the critical aspects of the SSPI design is the modularity wherein all modules are identical and made up of repeatable fundamental

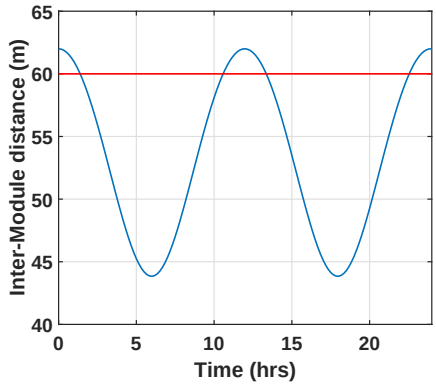

Figure 11. Variation of inter-module distance with time for two modules that are initially separated by a distance of 60 m. The red curve represents the ideal scenario of constant distance from antenna array efficiency point of view. This variation is due to the elliptical nature of PROs dictated by Equation 9.

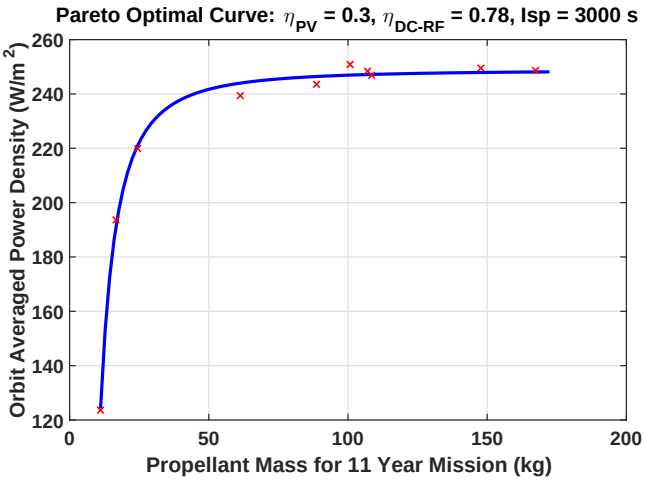

Figure 13. Pareto optimal curve for the worst case module in a constellation where the modules are in circularized, concentric periodic relative orbits. The propellant mass required is significantly lowered compared to the Pareto optimal curve shown in Fig. 10.

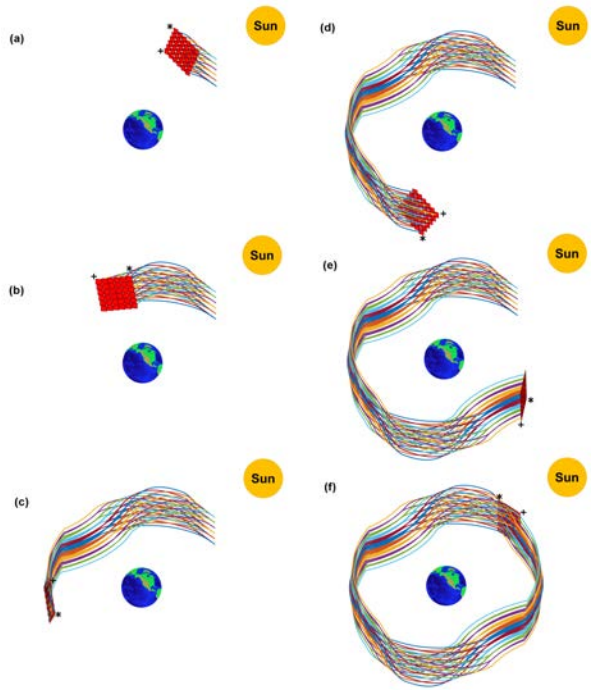

Figure 12. Orbits of a 6×6 constellation with modules in circularized periodic relative orbits. The plane of the constellation rotates continuously to optimize the efficiency of power generation and transmission. The positions of two of the modules are marked with $*$ and $+$ to help track their positions. These plots are from the point of view of an inertial observer over 24 hours. Note that the sizes of elements in this figure are not representative of their actual sizes.

units $i.e.$ tiles. It is hence imperative that all modules carry the same amount of propellant. In order to realize this goal, we propose to interchange the positions of the modules on a few occasions over the 11-year mission cycle so that on average, each module is approximately at the same distance from the geostationary orbit. The details of this interchange will be worked out in the future.

While our results indicate that modified periodic relative orbits offer a promising solution for designing a constellation for space-based solar power, numerous assumptions have been made in generating these initial results. In the future, the focus will be on understanding the effects of these assumptions and to further refine these orbits.

In this paper, we have only considered planar constellations. This was done in order to eliminate the possibility of modules shadowing each other. In the future, we intend to explore non-planar solutions that might require less propellant to deliver the same amount of orbit-averaged power. Depending on the experimentally realized values of areal mass density, the analysis will also be refined to include the effects of solar radiation pressure and other perturbations.

To deal with the challenge posed by varying inter-module distance, our initial approach has been to circularize the PROs. Some of the reduction in the performance of the array can be recovered by adjusting the relative phase of the modules. By exploring this trade-space further, we may be able to reduce the propellant mass being consumed for fully-circularizing the orbits. In the future, a script that computes the antenna array efficiency for different orbital configurations, adding appropriate phase-shift compensation, can be incorporated in the optimization framework.

It is important to also note that circularization of the orbits does not guarantee that the array is operating at its maximum efficiency. Since the circularization constraint is only imposed on the centers of the modules without taking into consideration the size and shape of the modules, as the modules go around the reference orbit, they go through phases where sections close to the corners of the modules start overlapping

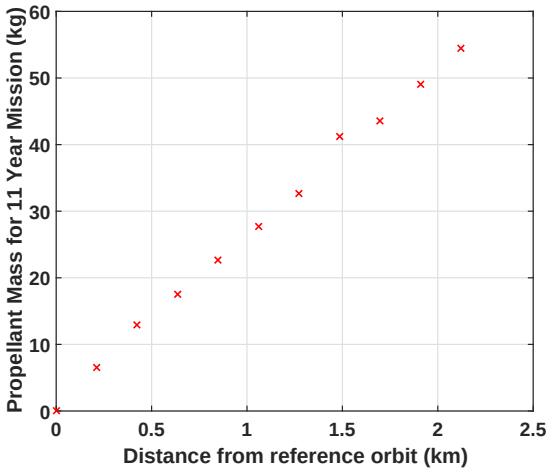

Figure 14. Variation of propellant mass with distance of module from the reference geostationary orbit. The behavior is largely linear and the small deviations are likely due to numerical fluctuations. Note that the data point corresponding to the highest fuel value on this plot was obtained for a module starting at $y = 1.5$ km and $z = 1.5$ km. This is same as the fourth data point on Fig. 13 which yields an orbit averaged power density of $240W/m^2$. In fact, all points in this figure yield the same orbit averaged power density.

each other. This effect can be seen in Fig. 12. This could have been avoided by rotating the modules about the local y-axis appropriately. However, due to restrictions imposed by the photovoltaic concentrators, the modules are only allowed to rotate about the z-axis in the LVLH frame. In the future, the effect of this overlap on the RF transmission efficiency will also be studied in more detail.

While the results have been presented for the baseline design of a constellation in GEO, these results can be easily extended in the future for constellations in low Earth orbit (LEO) or highly elliptical orbit (HEO).

6. CONCLUSIONS

In this paper, we have shown the optimum attitude profiles that help us establish theoretical limits on space-based solar power using planar modules. We also explained how these attitude maneuvers have to be accompanied by orbital maneuvers. Different strategies for carrying out these orbital maneuvers were discussed. Our results show that using modified, concentric periodic relative orbits is critical for keeping the propellant mass down to reasonable values. The thrust profiles obtained for both attitude and orbital maneuvers, serve as critical inputs in the structural design of the modules. The variations observed in the relative positions of the modules can help design the strategy for phasing operations of the antenna array. The numbers obtained for propellant mass and orbit averaged power density can be used to carry out an accurate cost-benefit analysis. Therefore, these results represent a critical step in the path towards realizing a space-based solar power system.

7. ACKNOWLEDGEMENTS

The authors thank Northrop Grumman Corporation for supporting this project. We also thank all other members of the SSPI team at Caltech for their valuable inputs. Nicolas Lee was supported during this work by a postdoctoral fellowship from the W. M. Keck Institute for Space Studies.

REFERENCES

[1] I. Asimov, "Reason," *I, Robot*, pp. 59–77, 1941.

[2] P. E. Glaser, "Power from the sun: its future," *Science*, vol. 162, no. 3856, pp. 857–861, 1968.

[3] A. Manan, L. Nicolas, and P. Sergio, *Ultralight Structures for Space Solar Power Satellites*, ser. AIAA SciTech. American Institute of Aeronautics and Astronautics, 2016. [Online]. Available: http://dx.doi.org/10.2514/6.2016-1950

[4] D. P. Scharf, F. Y. Hadaegh, and S. R. Ploen, "A survey of spacecraft formation flying guidance and control (part 1): guidance," in *American Control Conference, 2003. Proceedings of the 2003*, vol. 2, Conference Proceedings, pp. 1733–1739.

[5] D. P. Scharf, F. Hadaegh, and S. R. Ploen, "A survey of spacecraft formation flying guidance and control. part ii: control," in *American Control Conference, 2004. Proceedings of the 2004*, vol. 4, Conference Proceedings, pp. 2976–2985.

[6] K. T. Alfriend, S. R. Vadali, and H. Schaub, "Formation flying satellites: Control by an astrodynamicist," *Celestial Mechanics and Dynamical Astronomy*, vol. 81, no. 1-2, pp. 57–62, 2001.

[7] K. Alfriend, S. R. Vadali, P. Gurfil, J. How, and L. Breger, *Spacecraft formation flying: Dynamics, control and navigation*. Butterworth-Heinemann, 2009, vol. 2.

[8] E. Davis, C. Dunn, R. Stanton, and J. Thomas, "The grace mission: meeting the technical challenges," 2000.

[9] M. T. Zuber, D. E. Smith, D. H. Lehman, T. L. Hoffman, S. W. Asmar, and M. M. Watkins, "Gravity recovery and interior laboratory (grail): Mapping the lunar interior from crust to core," *Space Science Reviews*, vol. 178, no. 1, pp. 3–24, 2013.

[10] G. Krieger, A. Moreira, H. Fiedler, I. Hajnsek, M. Werner, M. Younis, and M. Zink, "Tandem-x: A satellite formation for high-resolution sar interferometry," *IEEE Transactions on Geoscience and Remote Sensing*, vol. 45, no. 11, pp. 3317–3341, 2007.

[11] E. Gill, O. Montenbruck, and S. D'Amico, "Autonomous formation flying for the prisma mission," *Journal of Spacecraft and Rockets*, vol. 44, no. 3, pp. 671–681, 2007. [Online]. Available: http://dx.doi.org/10.2514/1.23015

[12] D. Bock, M. Bethge, and M. Tajmar, "Highly miniaturized feep thrusters for cubesat applications," in *Proceedings of the 4th Spacecraft Propulsion Conference, Cologne*, vol. 2967498, Conference Proceedings.

[13] R. S. Legge and P. C. Lozano, "Electrospray propulsion based on emitters microfabricated in porous metals," *Journal of Propulsion and Power*, vol. 27, no. 2, pp. 485–495, 2011.

[14] J. P. Sheehan, T. A. Collard, F. H. Ebersohn, and B. W. Longmier, "Initial operation of the cubesat ambipolar

thruster," in *34th International Electric Propulsion Conference*, Conference Proceedings.

[15] P. Sheehan, T. Collard, B. W. Longmier, and I. Goglio, "New low-power plasma thruster for nanosatellites," in *Propulsion and Energy Forum. American Institute of Aeronautics and Astronautics*, Conference Proceedings.

[16] W. Clohessy and R. Wiltshire, "Terminal guidance system for satellite rendezvous," *Journal of the Aerospace Sciences*, vol. 27, no. 9, pp. 653–658, 1960.

[17] P. E. Gill, W. Murray, and M. A. Saunders, "Snopt: An sqp algorithm for large-scale constrained optimization," *SIAM review*, vol. 47, no. 1, pp. 99–131, 2005.

[18] D. P. Hamilton and A. V. Krivov, "Circumplanetary dust dynamics: Effects of solar gravity, radiation pressure, planetary oblateness, and electromagnetism," *Icarus*, vol. 123, no. 2, pp. 503–523, 1996.

[19] J. A. Atchison and M. A. Peck, "Length scaling in spacecraft dynamics," *Journal of guidance, control, and dynamics*, vol. 34, no. 1, pp. 231–246, 2011.

[20] R. G. Melton, "Time-explicit representation of relative motion between elliptical orbits," *Journal of Guidance, Control, and Dynamics*, vol. 23, no. 4, pp. 604–610, 2000.

[21] D. Morgan, S.-J. Chung, L. Blackmore, B. Acikmese, D. Bayard, and F. Y. Hadaegh, "Swarm-keeping strategies for spacecraft under j2 and atmospheric drag perturbations," *Journal of Guidance, Control, and Dynamics*, vol. 35, no. 5, pp. 1492–1506, 2012.

BIOGRAPHY

Ashish Goel *is currently a postdoctoral researcher at Caltech where he is working on the design of a formation flying constellation for Caltech's Space Solar Power Initiative. He is also developing flight electronics for a space mission to demonstrate the autonomous assembly and reconfiguration of a space telescope. He received his PhD in 2016 from Stanford University where we worked on developing sensors and systems for the detection and characterization of meteoroid and orbital debris impacts on satellites. He has also led the design teams for a Europa CubeSat project and a flight demonstration mission for a radioisotope thermophotovoltaic power source. In addition, he has been involved in numerous projects associated with high altitude balloon launches.*

Nicolas Lee *is an Engineering Research Associate in Aeronautics and Astronautics at Stanford University, after receiving a Ph.D. at Stanford University and a W. M. Keck Institute for Space Studies postdoctoral fellowship at Caltech. Current research interests include exploration of the space environment, asteroid resource utilization, deployable space structures, and small spacecraft systems.*

Sergio Pellegrino *received the Laurea degree in civil engineering from the University of Naples, Naples, Italy, in 1982, and the Ph.D. degree in structural mechanics from the University of Cambridge, Cambridge, U.K., in 1986. He served on the faculty of the University of Cambridge from 1985 to 2007 and he is currently the Joyce and Kent Kresa Professor of Aeronautics and a Professor of Civil Engineering with the California Institute of Technology, Pasadena, CA, USA, and a Jet Propulsion Laboratory Senior Research Scientist. His current research interests include the mechanics of lightweight structures, with a focus on packaging, deployment, shape control, and stability. With his students and collaborators, he is currently working on novel concepts for future space telescopes, spacecraft antennas, and space-based solar power systems. Dr Pellegrino is a Fellow of the Royal Academy of Engineering, a Fellow of AIAA and a Chartered Structural Engineer. He is President of the International Association for Shell and Spatial Structures (IASS) and has been the founding chair of the AIAA Spacecraft Structures Technical Committee. Dr Pellegrino has authored over 250 technical publications.*